28

Traffic Network Control Based on Hybrid System Modeling

Youngwoo Kim
Nagoya University, Nagoya
Japan

1. Introduction

With the increasing number of automobiles and complication of traffic network, the traffic flow control becomes one of significant economic and social issues in urban life. Many researchers have been involved in related researches in order to alleviate traffic congestion. From viewpoint of modeling, the existing scenarios can be categorized into the following two approaches:

(A1) Microscopic approach; and

(A2) Macroscopic approach.

The basic idea of Microscopic approach (A1) (2)is that the behavior of each vehicle is affected by neighboring vehicles, and the entire traffic flow is represented as statistical occurrences. The Cellular Automaton (CA) based model (3) (4) and (11) is widely known idea to represent the behavior of each vehicle. In the CA model, the road is discretized into many small cells. Each cell can be either empty or occupied by only one vehicle. The behavior of each vehicle in each cell is specified by the geometrical relationship with other vehicles together with some stochastic parameters. Although many simulation results based on these microscopic models showed high similarity to the measured real data, these approaches are not suitable for the large-scale traffic network modeling and its traffic light controller design. This is because they require enormous computational efforts to find all vehicles' behavior. Furthermore, the precise information on initial positions and speeds of all vehicles are usually not available in advance.
On the other hand, it has been a common strategy in the macroscopic approach (A2) (9) that the designer uses a fluid approximation model where the behavior of traffic flow is regarded as a continuous fluid with density $k(x,t)$ and volume $q(x,t)$ at location x and time t. In this case, $k(x,t)$ and $q(x,t)$ must satisfy the following law of mass conservation;

$$\frac{\partial k(x,t)}{\partial t} + \frac{\partial q(x,t)}{\partial x} = 0. \tag{1}$$

Also, some relationship among q, k and v, which are usually described by

$$q(x,t) = k(x,t)v(x,t), \tag{2}$$

is introduced together with the appropriate model of the $v(x,t)$, where $v(x,t)$ denotes the velocity of the traffic flow. By incorporating these two equations, the macroscopic behavior of

the traffic flow is uniquely decided. This model, however, is applicable only when the density of the traffic flow $k(x,t)$ is continuous. Although this model expresses well the behavior of the flow on the freeway, it is unlikely that this model can be applied to the urban traffic network which involves many discontinuities of the density coming from the existence of intersections controlled by traffic signals. In order to treat the discontinuity of the density in the macroscopic model, the idea of 'shock wave', which represents the progress of the boundary of two neighboring different density area, has been introduced in literature (6) (5) (7) (8). Although these approaches included judicious use of theoretical ideas for the flow dynamics, it is not straightforward to exploit them for the design of real-time traffic signal control since the flow model results in complicated nonlinear dynamics.

This paper presents a new method for the real-time traffic network control based on an integrated Hybrid Dynamical System (HDS) framework. The proposed method characterizes its synthetic modeling description. The information on geometrical traffic network is modeled by using Hybrid Petri Net (HPN), whereas the information on the behavior of traffic flow is modeled by means of Mixed Logical Dynamical Systems (MLDS) description. The former allows us to easily apply our method to complicated and wide range of traffic network due to its graphical understanding and algebraic manipulability. The latter allows us to represent physical features governing the dynamics of traffic flow and control mechanism for traffic congestion control employing the model predictive control policy (13).

Note that current traffic flow away from the signaler affects future traffic flow behavior. Through the model predictive control policy, we can construct the decentralized controller in a manner that each traffic outflow from the intersection or crosswalk is controlled and the information is shared with neighboring traffic controllers. A large-scale centralized traffic network controller is not appropriate because of the increased computational effort, synchronization in information processes and so on. In this case, the decentralized controller with model predictive control policy could be a realistic method.

In order to control large-scale traffic network with nonlinear dynamics, we formulate the traffic network control system based on the Mixed Integer NonLinear Programming (MINLP) problem. Generally, it is difficult to find the global optimal solution to the nonlinear programming problem. However, if the problem can be recast to the convex programming problem, the global optimal solution is easily found by applying an efficient method such as Steepest Descent Method (SDM). We use in this paper general performance criteria for traffic network control and show that although the problem contains non-convex constraint functions as a whole, the generated sub-problems are always included in the class of convex programming problem. In order to achieve high control performance of the traffic network with dynamically changing traffic flow, we adopt Model Predictive Control (MPC) policy. Note that MLDS formulation often encounters multiplication of two decision variables, and that without modification, it cannot be directly applied to MPC scheme. One way to avoid the multiplication is to introduce a new auxiliary variable to represent it. And then it becomes a linear system formally. However, as we described before, the introduction of discrete variables causes substantial computational amounts. A new method for this type of control problem is proposed. Although the system representation is nonlinear, MPC policy is successfully applied by means of the proposed Branch and Bound strategy.

After verification of the solution optimality, PWARX classifier is applied which describes a nonlinear feedback control law of the traffic control system. This implies we don't need a time-consuming searching process of a solver such as a Branch-and-Bound algorithm to solve

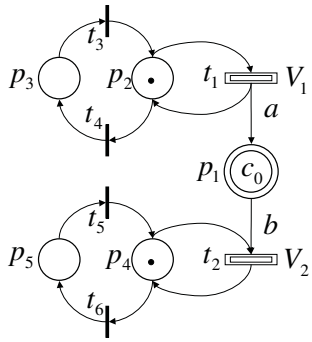

Fig. 1. Example of Hybrid Petri Net model

a mixed integer nonlinear programming (MINLP) problem, and furthermore the exactly same solutions are obtained in a very short time.

The problem we address in this paper is a special classification problem where the output y is a 0-1 binary variable, and very good classification performance is desirable even with very large number of the introduced clusters. If we plot the observational data in a same cluster in the x-y space, it will show always zero inclination, since we have a binary output, i.e., all components of θ, a and b except for f will be zeros. This implies we need consideration for a binary output. A new performance criterion is presented in this paper to consider not only a covariance of θ, but also a covariance of y. The proposed method is a hierarchical classification procedure, where the cluster splitting process is introduced to the cluster with the worst classification performance (which includes 0-1 mixed values of y). The cluster splitting process is follows by the piecewise fitting process to compute the cluster guard and dynamics, and the cluster updating process to find new center points of the clusters. The usefulness of the proposed method is verified through some numerical experiments.

2. Modeling of Traffic Flow Control System (TFCS) based on HPN

The Traffic Flow Control System (TFCS) is the collective entity of traffic network, traffic flow and traffic signals. Although some of them have been fully considered by the previous studies, most of the previous studies did not simultaneously consider all of them. In this section, the HPN model is developed, which provides both graphical and algebraic descriptions for the TFCS.

2.1 Representation of TFCS as HPN

HPN is one of the useful tools to model and visualize the system behavior with both continuous and discrete variables. HPN is a structure of $N = (P, T, I_+, I_-, C, D)$. The set of places P is partitioned into a subset of discrete places P_d and a subset of continuous places P_c. The set of transition T is partitioned into a subset of discrete transitions T_d and a subset of continuous transitions T_c. The incidence matrix of the net is defined as $I(p,t) = I_-(p,t) - I_+(p,t)$, where $I_+(p,t)$ and $I_-(p,t)$ are the forward and backward incidence relationships between the transition t and the place p which follows and precedes the transition. We denote the preset (postset) of transition t as $^\bullet t$ ($t^\bullet$) and its restriction to continuous or discrete places as $^{(d)}t =$

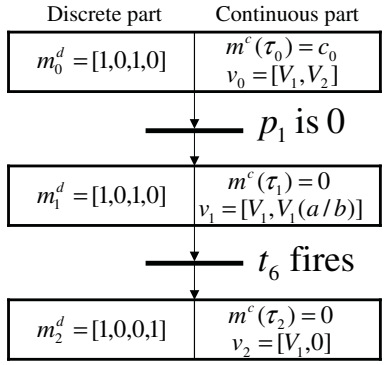

Fig. 2. Phase diagram of Hybrid Petri Net model

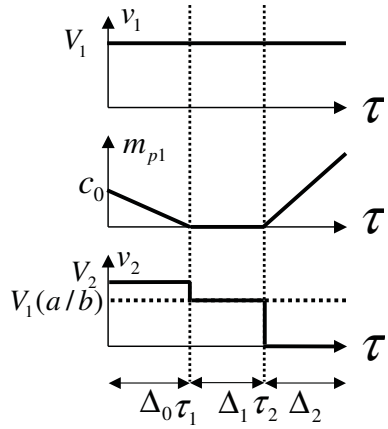

Fig. 3. Behavior of Hybrid Petri Net model

$^\bullet t \cap P_d$ or $^{(c)}\ t = {}^\bullet t \cap P_c$. Similar notation may be used for presets and postsets of places. The function C and D specify the firing speeds associated to the continuous transitions and the timing associated to the (timed) discrete transitions. For any continuous transition t_i, we let $C(t_i) = (v_i, V_i)$, where v_i and V_i represent the minimum and maximum firing speed of transition t_i. We associate to the timed discrete transition its firing delay, where the firing delay is short enough and the state is preserved until next sampling instant. The acquisition of firing sequence of the discrete transition at every sampling instant is applied to a variety of scheduling and control problems. The marking $M = [M_C|M_D]$ has both continuous (m dimension) and discrete (n dimension) parts.

Consider a simple example of First-Order Hybrid Petri Net model, Fig.1, where the control switch is represented with two discrete transitions and two discrete places connected to the continuous transition. In Fig.1, p_1 is the continuous place with the initial marking $m_c(\tau_0) = m_{p1} = c_0$, and p_2, p_3, p_4 and p_5 are the discrete places with the initial marking $m_d(\tau_0) = [m_{p2}, m_{p3}, m_{p4}, m_{p5}] = [1, 0, 1, 0]$. We assume $V_1 a < V_2 b$, where V_1 and V_2 are firing speed of t_1 and

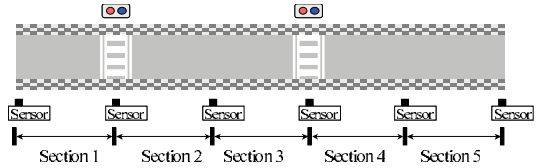

Fig. 4. Traffic network

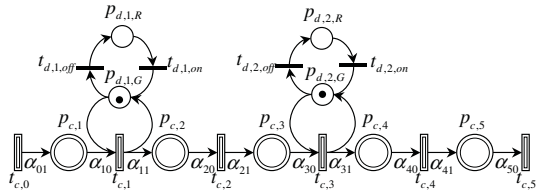

Fig. 5. Hybrid Petri Net model of traffic network

t_2 respectively, a and b are the arc weights given by the incidence relationship. The behavior is illustrated in Fig.2 and Fig.3.

Figure 5 shows the HPN model for the road of Fig.4. In Fig.5, each section i of l_i-meters long constitutes the straight road, and two traffic lights are installed at the point of crosswalk. $p_c \in P_c$ represents each section of the road, and has maximum capacity (maximum number of vehicles). Also, $p_d \in P_d$ represents the traffic signal where green signal is indicated by an existence of a token. Note that each signal is supposed to have only two states 'go (green)' or 'stop (red)' for simplicity.T is the set of continuous transitions which represent the boundary of two successive sections. $q_j(\tau)$ is the firing speeds assigned to transition $t_j \in T$ at time τ. $q_j(\tau)$ represents the number of vehicles passing through the boundary per time unit of two successive sections(measuring position) at time τ. The sensors to capture the number of the vehicles are supposed to be installed at every boundary of the section as show in Fig.4. The element of $I(p,t)$ is always 0 or α_{ij}. α_{ij} is the number of traffic lanes in each section. Finally, M^0 is specified as the initial marking of the place $p \in P$. The net dynamics of HPN is represented by a simple first order differential equation for each continuous place $p_{c_i} \in P_c$ as follows:

if $p_{d,k} = {}^\bullet t_j$ is not null,

$$\frac{dm_{C,i}(\tau)}{dt} = \sum_{t_j \in p_{c_i}{}^\bullet \cup {}^\bullet p_{c_i}} I(p_{c_i}, t_j) \cdot q_j(\tau) \cdot m_{D,k}(\tau), \tag{3}$$

otherwise,

$$\frac{dm_{C,i}(\tau)}{dt} = \sum_{t_j \in p_{c_i}{}^\bullet \cup {}^\bullet p_{c_i}} I(p_{c_i}, t_j) \cdot q_j(\tau), \tag{4}$$

where $m_{C,i}(\tau)$ is the marking for the place $p_{c_i} (\in P_c)$ at time τ, and $m_{D,k}(\tau)$ is the marking for the place $p_{d_k} (\in P_d)$. The equation (3) is transformed to its discrete-time version supposing

that $q_j(\tau)$ is constant during two successive sampling instants as follows:

$$m_{C,i}((\kappa+1)T_s) = m_{C,i}(\kappa T_s) + \sum_{t_j \in p_{c_i}{}^{\bullet} \cup {}^{\bullet} p_{c_i}} I(p_{c_i}, t_j) \cdot q_j(\kappa T_s) \cdot m_{D,j}(\kappa T_s) \cdot T_s. \quad (5)$$

where κ is sampling index, and T_s is sampling period.
Note that the transition t is *enabled* at the sampling instant κT_s if the marking of its preceding discrete place $p_{d_j} \in P_d$ satisfies $m_{D,j}(\kappa) \geq I_+(p_{d_j}, t)$. Also if t does not have any input (discrete) place, t is always *enabled*.

2.2 Definition of flow q_i

In order to derive the flow behavior, the relationship among $q_i(\tau)$, $k_i(\tau)$ and $v_i(\tau)$ must be specified. One of the simple ideas is to use the well-known model

$$q_i(\tau) = \frac{(k_i(\tau) + k_{i+1}(\tau))}{2} \frac{v_i(\tau) + v_{i+1}(\tau)}{2} \quad (6)$$

supposing that the density $k_i(\tau)$ and $k_{i+1}(\tau)$, and average velocity $v_i(\tau)$ and $v_{i+1}(\tau)$ of the flow in i and $(i+1)$th sections are almost identical. Then, by incorporating the velocity model

$$v_i(\tau) = v_{f_i} \cdot \left(1 - \frac{k_i(\tau)}{k_{jam}}\right), \quad (7)$$

with (6), the flow dynamics can be uniquely defined. Here, k_{jam} is the density in which the vehicles on the roadway are spaced at minimum intervals (traffic-jammed), and v_{f_i} is the maximum speed, that is, the velocity of the vehicle when no other vehicle exists in the same section.
If there exists no abrupt change in the density on the road, this model is expected to work well. However, in the urban traffic network, this is not the case due to the existence of the intersections controlled by the traffic signals. In order to treat the discontinuities of the density among neighboring sections (i.e. neighboring continuous places), the idea of 'shock wave'(10) is introduced as follows. We consider the case as shown in Fig.6 where the traffic density of ith section is lower than that of $(i+1)$th section in which the boundary of density difference designated by the dotted line is moving forward. Here, the movement of this boundary is called shock wave and the moving velocity of the shock wave $c_i(\tau)$ depends on the densities and average velocities of ith and $(i+1)$th sections as follows:

$$c_i(\tau) = \frac{v_i(\tau)k_i(\tau) - v_{i+1}(\tau)k_{i+1}(\tau)}{k_i(\tau) - k_{i+1}(\tau)}. \quad (8)$$

The traffic situation can be categorized into the following four types taking into account the density and shock wave.

(C1) $k_i(\tau) < k_{i+1}(\tau)$, and $c_i(\tau) > 0$,

(C2) $k_i(\tau) < k_{i+1}(\tau)$, and $c_i(\tau) \leq 0$,

(C3) $k_i(\tau) > k_{i+1}(\tau)$,

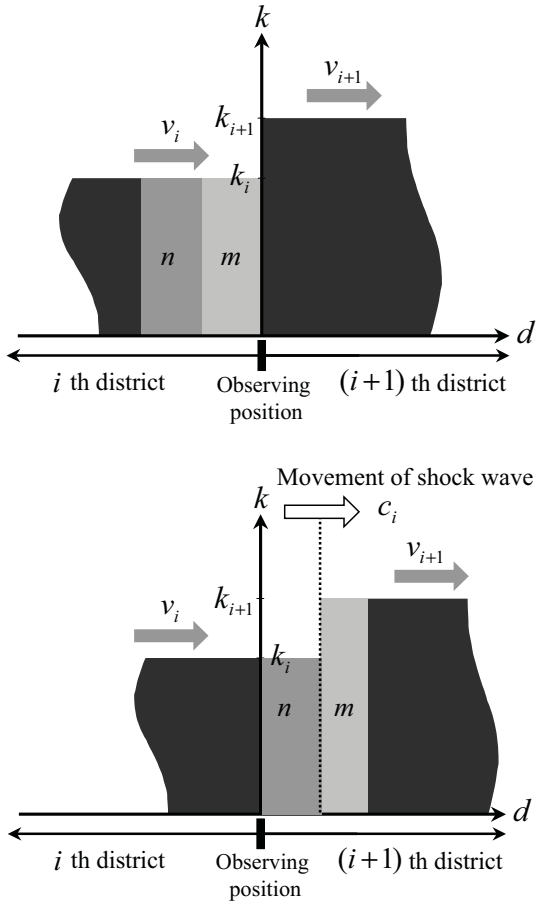

Fig. 6. Movement of shock wave in the case of $k_i(\tau) < k_{i+1}(\tau)$ and $c_i(\tau) > 0$

(C4) $k_i(\tau) = k_{i+1}(\tau)$ (no shock wave).

Firstly, in both cases of (C1) and (C2) where $k_i(\tau)$ is smaller than $k_{i+1}(\tau)$, the vehicles passing through the density boundary (dotted line) reduce their speeds. The movement of the shock wave is illustrated in Fig.6 ($c_i(\tau) > 0$) and Fig.7 ($c_i(\tau) \leq 0$). In Fig.6 and Fig.7, the 'measuring position' implies the position where transition t_i is assigned. Since the traffic flow $q_i(\tau)$ represents the numbers of vehicles passing through the measuring position per unit time, in the case of (C1), it can be represented by $n + m$ in Fig.6, where n and m represent the area of the corresponding rectangular, i.e. the product of the $v_i(\tau)$ and $k_i(\tau)$. Similarly, in the case of (C2), $q_i(\tau)$ can be represented by m in Fig.7.
These considerations lead to the following models:

in the case of (C1)

$$q_i(\tau) = v_i(\tau)k_i(\tau) \tag{9}$$

$$= v_{f_i}\left(1 - \frac{k_i(\tau)}{k_{jam}}\right)k_i(\tau), \tag{10}$$

in the case of (C2)

$$q_i(\tau) = v_{i+1}(\tau)k_{i+1}(\tau) \tag{11}$$

$$= v_{f_{i+1}}\left(1 - \frac{k_{i+1}(\tau)}{k_{jam}}\right)k_{i+1}(\tau). \tag{12}$$

In the cases of (C3) and (C4) where $k_i(\tau)$ is greater than $k_{i+1}(\tau)$, the vehicles passing through the density boundary come to accelerate. In this case, the flow can be well approximated by taking into account the average density of neighboring two sections. This is intuitively because the difference of the traffic density is going down. Then in the cases of (C3) and (C4), the traffic flow can be formulated as follows:

in the cases of (C3) and (C4),

$$q_i(\tau) = \left(\frac{k_i(\tau) + k_{i+1}(\tau)}{2}\right)v_f(\tau)\left(1 - \frac{k_i(\tau) + k_{i+1}(\tau)}{2k_{jam}}\right). \tag{13}$$

As the results, the flow model (9) $\sim$ (13) taking into account the discontinuity of the density can be summarized as follows:

$$q_i(\tau) = \begin{cases} \left(\frac{k_i(\tau)+k_{i+1}(\tau)}{2}\right)v_f\left(1 - \frac{k_i(\tau)+k_{i+1}(\tau)}{2k_{jam}}\right) \\ \quad if\ k_i(\tau) \geq k_{i+1}(\tau) \\ v_{f_i}\left(1 - \frac{k_i(\tau)}{k_{jam}}\right)k_i(\tau) \\ \quad if\ k_i(\tau) < k_{i+1}(\tau) \text{ and } c(\tau) > 0 \\ v_{f_{i+1}}\left(1 - \frac{k_{i+1}(\tau)}{k_{jam}}\right)k_{i+1}(\tau) \\ \quad if\ k_i(\tau) < k_{i+1}(\tau) \text{ and } c(\tau) \leq 0 \end{cases}. \tag{14}$$

Figure 8 shows the HPN model of the ith intersection, where the notation for other than southwardly entrance lane is omitted. In Fig.8, $l_{j,E}$, $l_{j,W}$, $l_{j,S}$ and $l_{j,N}$ are the length of the corresponding districts, and the numbers of the vehicles in the districts are obtained as for example $p_{c,j_{IS}}(\tau) = k_{j_{IS}}(\tau) \cdot l_{j,S}$. The vehicles in $p_{c,j_{IS}}$ are assumed to have the probability $\zeta_{j,SW}$, $\zeta_{j,SN}$, and $\zeta_{j,SE}$ to proceed into the district corresponding to $p_{c,j_{OW}}$, $p_{c,j_{ON}}$, and $p_{c,j_{OE}}$ as follows,

$$k_{j_{SW}}(\tau) = k_{j_{IS}}(\tau)\zeta_{j,SW}(\tau), \tag{15}$$

$$k_{j_{SN}}(\tau) = k_{j_{IS}}(\tau)\zeta_{j,SN}(\tau), \tag{16}$$

$$k_{j_{SE}}(\tau) = k_{j_{IS}}(\tau)\zeta_{j,SE}(\tau). \tag{17}$$

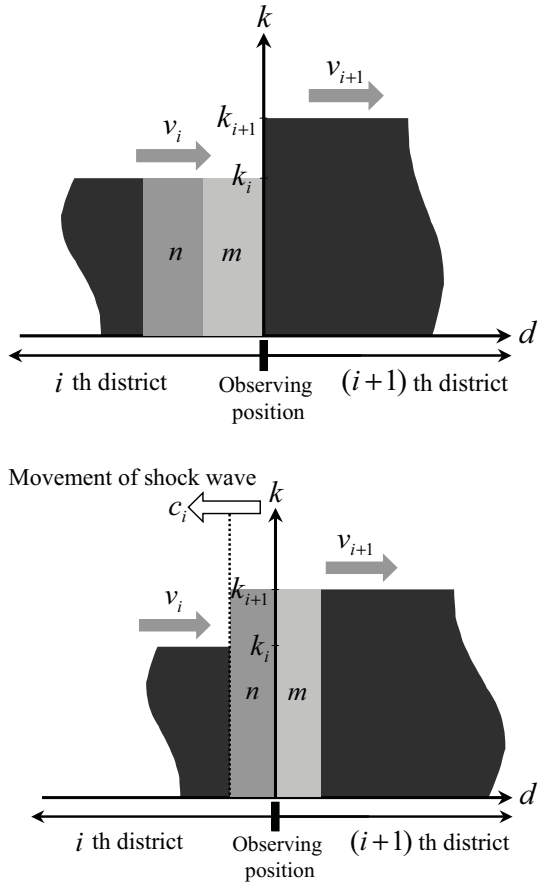

Fig. 7. Movement of shock wave in the case of $k_i(\tau) < k_{i+1}(\tau)$ and $c_i(\tau) \leq 0$

Note that these probabilities are determined by the traffic network structure, and satisfy at τ,

$$0 \leq \zeta_{j,SW}(\tau) \leq 1, \tag{18}$$
$$0 \leq \zeta_{j,SN}(\tau) \leq 1, \tag{19}$$
$$0 \leq \zeta_{j,SE}(\tau) \leq 1, \tag{20}$$
$$\zeta_{j,SW}(\tau) + \zeta_{j,SN}(\tau) + \zeta_{j,SE}(\tau) = 1. \tag{21}$$

Therefore, the traffic flows of the three directions are represented with

$$q\left(k_{j_{SN}}(\tau), k_{j_{ON}}(\tau)\right), \tag{22}$$
$$q\left(k_{j_{SW}}(\tau), k_{j_{OW}}(\tau)\right), \tag{23}$$
$$q\left(k_{j_{SE}}(\tau), k_{j_{OS}}(\tau)\right). \tag{24}$$

Note that the mutual exclusion of the same traffic light with the intersecting road is represented in the Fig.8.

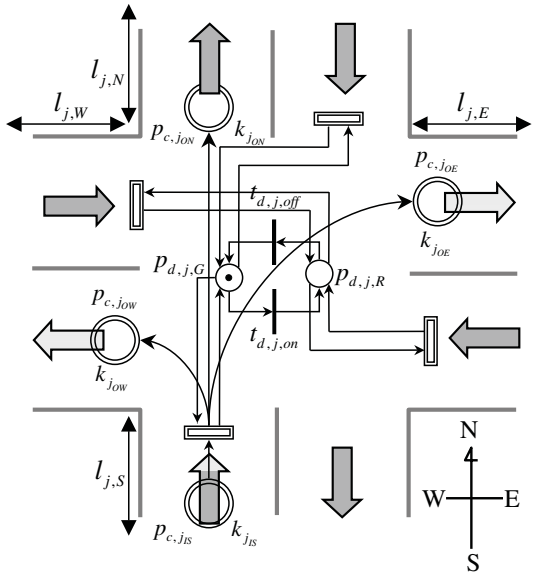

Fig. 8. Hybrid Petri Net model of intersection

2.3 Derived flow model

In this subsection, we confirm the effectiveness of the proposed traffic flow model developed in the previous subsection by comparing it with the microscopic model. The usefulness of Cellular Automaton (CA) in representing the traffic flow behavior was investigated in (3). Some of well-known traffic flow simulators such as TRANSIMS and MICROSIM are based on CA model.

The essential property of CA is characterized by its lattice structure where each cell represents a small section on the road. Each cell may include one vehicle or not. The evolution of CA is described by some rules which describe the evolution of the state of each cell depending on the states of its adjacent cells.

The evolution of the state of each cell in CA model can be expressed by

$$n_j(\tau+1) = n_j^{in}(\tau)(1-n_j(\tau)) - n_j^{out}(\tau), \tag{25}$$

where $n_j(\tau)$ is the state of cell j which represents the occupation by the vehicle ($n_j(\tau) = 0$ implies that the jth cell is empty, and $n_j(\tau) = 1$ implies that a vehicle is present in the jth cell at τ). $n_j^{in}(\tau)$ represents the state of the cell from which the vehicle moves to the jth cell, and $n_j^{out}(\tau)$ indicates the state of the destination cell leaving from the jth cell. In order to find $n_j^{in}(\tau)$ and $n_j^{out}(\tau)$, some rules are adopted as follows:

Step 1, Acceleration rule: All vehicles, that have not reached at the speed of maximum speed v_f, accelerate its speed $v_{\langle j\rangle}(\tau)$ by one unit velocity v_{unit} as follows:

$$v_{\langle j\rangle}(\tau+\Delta\tau) \equiv v_{\langle j\rangle}(\tau) + v_{unit}. \tag{26}$$

Step 2, Safety distance rule: If a vehicle has e empty cells in front of it, then the velocity at the next time instant $v_{\langle j \rangle}(\tau + \Delta\tau)$ is restricted as follows:

$$v_{\langle j \rangle}(\tau + \Delta\tau) \equiv \min\{e, v_{\langle j \rangle}(\tau + \Delta\tau)\}. \tag{27}$$

Step 3, Randomization rule: With probability p, the velocity is reduced by one unit velocity as follows:

$$v_{\langle j \rangle}(\tau + \Delta\tau) \equiv v_{\langle j \rangle}(\tau + \Delta\tau) - p \cdot v_{unit}. \tag{28}$$

Figure 9 shows the behavior of traffic flow obtained by applying the CA model to the two successive sections which is 450[m] long. The parameters used in the simulation are as follows: computational interval $\Delta\tau$ is 1 [sec], each cell in the CA is assigned to 4.5 [m]-long interval on the road, maximum speed v_f is 5 (cells/$\Delta\tau$), which is equivalent to 81 [Km/h] (=4.5[m/cell] $\cdot$ 5 [cells/$\Delta\tau$] $\cdot$ 3600[sec]/1000). The left figure of Fig.9 shows the obtained relationship among normalized flow $q_i(\tau)$ and densities $k_i(\tau)$ and $k_{i+1}(\tau)$. The right small figure is the abstracted illustration of the real behavior.
First of all, we look at the behavior along the edge a in the right figure which implies the case that the traffic signal is changed from red to green. At the point of $k_i(\tau) = 0$ and $k_{i+1}(\tau) = 0$, the traffic flow $q_i(\tau)$ becomes zero since there is no vehicle in both ith and $(i+1)$th section. Then, $q_i(\tau)$ is proportionally increased as $k_i(\tau)$ increases, and reaches the saturation point ($k_i(\tau) = 0.9$). Next, we look at the behavior along the edge b which implies that the ith section is fully occupied. In this case, the maximum flow is measured until the density of the $(i+1)$th section is reduced by 50% (i.e. $k_{i+1}(\tau) = 0.5$), and after that the flow goes down according to the increase of $k_{i+1}(\tau)$. Although CA model consists of quite simple procedures, it can show quite natural traffic flow behavior.
On the other hand, Fig.10 shows the behavior in case of using HPN where the proposed flow model given by (14) is embedded. We can see that Fig.10 shows the similar characteristics to Fig.9, especially, the saturation characteristic is well represented despite of the use of macroscopic model. As another simple modeling strategy, we consider the case that the average of two $k_i(\tau)$ and $k_{i+1}(\tau)$ are used to decide the flow $q_i(\tau)$ (i.e. use (13)) for all cases. Figure 11 shows the behavior in case of using HPN where the flow model is supposed to be given by (13) for all cases. Although the $q_i(\tau)$ shows similar characteristics in the region of $k_i(\tau) \geq k_{i+1}(\tau)$, at the point of $k_i(\tau) = 0$ and $k_{i+1}(\tau) = k_{jam}$, $q_i(\tau)$ takes its maximum value. This obviously contradicts to the natural flow behavior.
Before concluding this subsection, it is worthwhile to compare the computational amount. In case of using CA, it took 140 seconds to construct the traffic flow dynamics using Athlon XP 2400 and Windows 2000, while only 0.06 seconds in case of using HPN and (14).

3. Model Predictive Control of Traffic Network Control based on MLDS description

The Receding Horizon Control (RHC) or Model Predictive Control (MPC) is one of well - known paradigms for optimizing the systems with constraints and uncertainties. In RHC paradigms, the solutions are elements of finite dimensional vector spaces, and finite-horizon optimization is carried out in order to provide stability or performance analysis. However, the application of RHC has been mainly restricted to the system with sufficiently long sampling interval, since finite-horizon optimization is computationally demanding.
This chapter firstly formulate the traffic flow model developed in chapter 2 in the form of MLDS description coupled with RHC strategy, where wide range of traffic flow is considered.

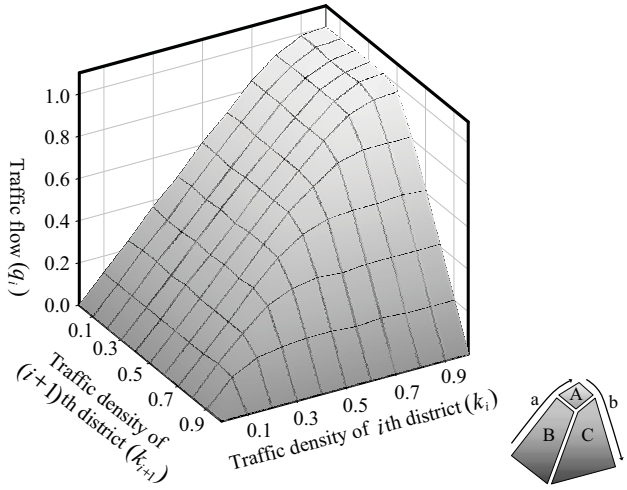

Fig. 9. Traffic flow behavior obtained from CA model

This formulation is recast to the canonical form of 0-1 Mixed Integer Linear Programming (MILP) problem to optimize its behavior and a new Branch and Bound (B&B) based algorithm is presented in order to abate computational cost of MILP problem.

3.1 MLDS representation of TCCS based on Piece-Wise Affine (PWA) linearization of traffic flow

Since TCCS is the hybrid dynamical system including both continuous traffic flow dynamics and discrete aspects for traffic light signal control, some algebraic formulation, which handles both continuous and discrete behaviors, must be introduced. The MLDS description has been developed to describe such class of systems considering some constraints shown in the form of inequalities and can be combined with powerful search engine such as Mixed Integer Linear Programming (MILP).
The MLDS (12) description can be formalized as following.

$$\begin{aligned} \boldsymbol{x}(\tau+1) &= \boldsymbol{A_\tau x}(\tau) + \boldsymbol{B_{1\tau}u}(\tau) \\ &\quad + \boldsymbol{B_{2\tau}}\delta(\tau) + \boldsymbol{B_{3\tau}}z(\tau) \qquad (29) \\ \boldsymbol{y}(\tau) &= \boldsymbol{C_\tau x}(\tau) + \boldsymbol{D_{1\tau}u}(\tau) \\ &\quad + \boldsymbol{D_{2\tau}}\delta(t) + \boldsymbol{D_{3\tau}}(\tau) \qquad (30) \\ \boldsymbol{E_{2\tau}}\delta(\tau) &+ \boldsymbol{E_{3\tau}}z(\tau) \leq \\ &\quad \boldsymbol{E_{1\tau}u}(\tau) + \boldsymbol{E_{4\tau}x}(\tau) + \boldsymbol{E_{5\tau}} \qquad (31) \end{aligned}$$

In MLDS formulation, (29), (30) and (31) are state equation, output equation and constraint inequality, respectively, where x, y and u are the state, output and input variable, whose components are constituted by continuous and/or 0-1 binary variables, $\delta(\tau) \in \{0, 1\}$ and $z(\tau) \in \Re$

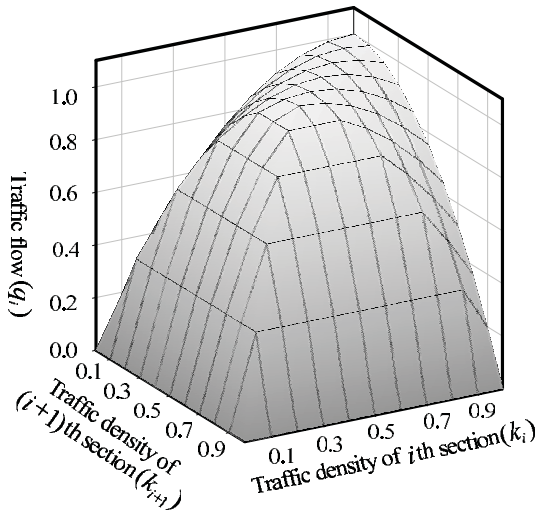

Fig. 10. Traffic flow behavior obtained from the proposed traffic flow model

represent auxiliary logical and continuous variables. By introducing the constraint inequality of (31), non-linear constraints as (14) can be transformed to the computationally tractable Piece-Wise Affine (PWA) forms.
The traffic flow of Fig. 9 can be approximated as the right figure of Fig. 9 which consists of three planes as follows,

Plane A: The traffic flow q_i is saturated ($k_i(\tau) \leq a$ and $k_{i+1}(\tau) < (k_{jam} - a)$)

Plane B: The traffic flow q_i is mainly affected by the quantity of traffic density $k_i(\tau)$ ($k_i(\tau) < a$ and $k_i(\tau) + k_{i+1} < k_{jam}$)

Plane C: The traffic flow q_i is mainly affected by the quantity of traffic density $k_{i+1}(\tau)$ ($k_{i+1}(\tau) \leq k_{jam} - a$ and $k_i(\tau) + k_{i+1} \leq k_{jam}$)

where a is the threshold value to describe saturation characteristic of traffic flow that if $k_i(\tau) > a$ and/or $k_{i+1}(\tau) < k_{jam} - a$, the value of $q_i(\tau)$ hovers at its maximum value q_{max}.

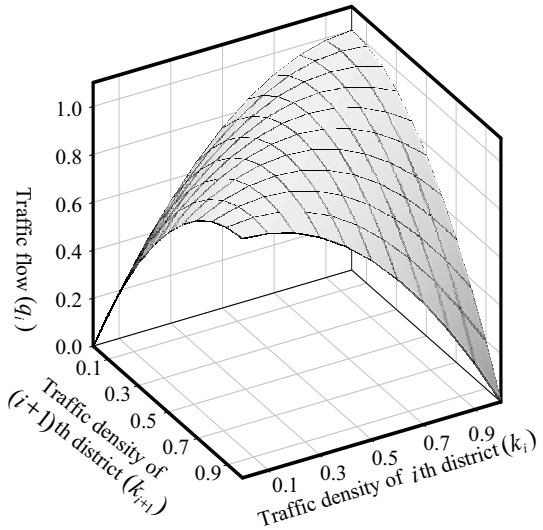

Fig. 11. Traffic flow behavior obtained by averaging k_i and k_{i+1}

Fig.12 shows three planes partitioned by introducing three auxiliary variables $\delta_{P,i,1}(\tau)$, $\delta_{P,i,2}(\tau)$ and $\delta_{P,i,3}(\tau)$ which are defined as follows,

$$[\delta_{P,i,1}(\tau) = 1] \leftrightarrow \begin{cases} k_i(\tau) & \geq & a \\ k_{i+1}(\tau) & \leq & k_{jam} - a \end{cases} \tag{32}$$

$$[\delta_{P,i,2}(\tau) = 1] \leftrightarrow \begin{cases} k_i(\tau) & \leq & a - \varepsilon \\ k_i(\tau) + k_{i+1}(\tau) & \leq & k_{jam} \end{cases} \tag{33}$$

$$[\delta_{P,i,3}(\tau) = 1] \leftrightarrow \begin{cases} k_{i+1}(\tau) & \geq & k_{jam} - a + \varepsilon \\ k_i(\tau) + k_{i+1}(\tau) & \geq & k_{jam} + \varepsilon \end{cases} \tag{34}$$

$$\delta_{P,i,1}(\tau) + \delta_{P,i,2}(\tau) + \delta_{P,i,3}(\tau) = 1 \tag{35}$$

where ε is small tolerance to consider equality sign.
Therefore, the traffic flow $q_i(\tau)$ can be rewritten in a compact form as follows

$$\begin{aligned} q_i(\tau) &= q_{max}\delta_{P,i,1}(\tau) + \frac{q_{max}k_i(\tau)}{a}\delta_{P,i,2}(\tau) \\ &\quad + \frac{q_{max}(1 - k_{i+1}(\tau))}{a}\delta_{P,i,3}(\tau) \end{aligned} \tag{36}$$

$$\sum_{i=1}^{3} \delta_{P,i,j}(\tau) = 1$$

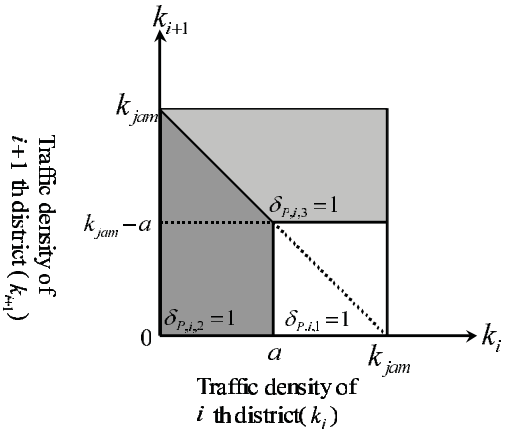

Fig. 12. Assignation of planes by introducing auxiliary variables

where $0 \leq k_i(\tau) \leq k_{jam}$, $0 \leq k_{i+1} \leq k_{jam}$ $(= 1)$, q_{max} is the maximum value of traffic flow. Figure xxx shows the piece-wise affine (PWA) dynamics of the traffic flow model developed in the previous chapter where $a = 0.3$ and $q_{max} = 1$.
The equations (32) to (34) can be generalized as (37) and (38), and transformed to inequality as (39) The equations (32) and (34) can be generalized as (37) and (38), and transformed to inequality as (39)

$$[\delta_{P,i,j}(\tau) = 1] \quad \leftrightarrow \quad \left[\begin{bmatrix} k_i \\ k_{i+1} \end{bmatrix} \in \ell_j \right] \tag{37}$$

$$\ell_j \quad = \quad \left\{ \begin{bmatrix} k_i \\ k_{i+1} \end{bmatrix} : \boldsymbol{S_j k_i}(\tau) \leq \boldsymbol{T_j} \right\} \tag{38}$$

where $\boldsymbol{k_i}(\tau) = [k_i(\tau) k_{i+1}(\tau)]^T$ and $\boldsymbol{S_j}$ and $\boldsymbol{T_j}$ are the matrices with suitable dimensions which satisfy

$$\boldsymbol{S_j k_i}(\tau) \quad - \quad \boldsymbol{T_j} \leq \boldsymbol{M_j}^*[1 - \delta_{P,i,j}(\tau)], \tag{39}$$

$$\boldsymbol{M_j^*} \quad \stackrel{\triangle}{=} \quad \max_{\boldsymbol{k_i} \in \ell_j} \boldsymbol{S_j k_i(\tau)} - \boldsymbol{T_j}. \tag{40}$$

The traffic flow $q_i(\tau)$ of (37) is the relationship between $\boldsymbol{k_i}(\tau)$ and $\boldsymbol{\delta_{P,i}}(\tau) = [\delta_{P,i,1}(\tau)\ \delta_{P,i,2}(\tau)\ \delta_{P,i,3}(\tau)]$ which can be rewritten as follows,

$$q_i(\tau) \quad = \quad f(\boldsymbol{\delta_{P,i}}(\tau), \boldsymbol{k_{i+1}}(\tau)) \tag{41}$$

$$\quad = \quad \sum_{j=1}^{3} (\boldsymbol{F_i^j}(\tau)\boldsymbol{k_i}(\tau) + \boldsymbol{H_i^j})\delta_{P,i,j}(\tau) \tag{42}$$

where $\boldsymbol{\delta_{P,i}} = [\delta_{P,i,1}, \delta_{P,i,2}, \delta_{P,i,3}]'$. In these equations, each pair of $\boldsymbol{F_i^j}$ and $\boldsymbol{H_i^j}$ represents the corresponding domain of Fig. 12 as follows,

$$\begin{aligned}
\boldsymbol{F_i^1} &= [\ 0 \quad 0\ ] && (43)\\
\boldsymbol{H_i^1} &= q_{max} && (44)\\
\boldsymbol{F_i^2} &= [\ \tfrac{q_{max}}{a} \quad 0\ ] && (45)\\
\boldsymbol{H_i^2} &= 0 && (46)\\
\boldsymbol{F_i^3} &= [\ 0 \quad -\tfrac{q_{max}}{a}\ ] && (47)\\
\boldsymbol{H_i^3} &= \frac{q_{max}}{a} && (48)
\end{aligned}$$

The traffic flow $\boldsymbol{z_i}(\tau) = [z_{i,1}(\tau)\ z_{i,2}(\tau)\ z_{i,3}(\tau)]$ in consideration of the binary input $u_i(\tau) \in \{0,1\}$ for traffic light control can be represented by

$$\begin{aligned}
z_{i,j}(\tau) &\leq M_i u_i(\tau)\delta_{P,i,j}(\tau), && (49)\\
z_{i,j}(\tau) &\geq m_i u_i(\tau)\delta_{P,i,j}(\tau), && (50)\\
z_{i,j}(\tau) &\leq \boldsymbol{F_i^j k_i}(\tau) + \boldsymbol{H_i^j} \\
&\quad -m_i(1-u_i(\tau)\delta_{P,i,j}(\tau)), && (51)\\
z_{i,j}(\tau) &\geq \boldsymbol{F_i^j k_i}(\tau) + \boldsymbol{H_i^j} \\
&\quad -M_i(1-u_i(\tau)\delta_{P,i,j}(\tau)). && (52)
\end{aligned}$$

where M_i and m_i are respectively

$$\begin{aligned}
M_i &= \max_{\boldsymbol{k_i}(\tau)\in\ell_j} \left\{ \boldsymbol{F_i^j k_i}(\tau) + \boldsymbol{H_j} \right\}, && (53)\\
m_i &= \min_{\boldsymbol{k_i}(\tau)\in\ell_j} \left\{ \boldsymbol{F_i^j k_i}(\tau) + \boldsymbol{H_j} \right\}. && (54)
\end{aligned}$$

The product $u_i(\tau)\ \delta_{P,i,j}(\tau)$ can be replaced by an auxiliary logical variable $\delta_{M,i,j}(\tau) = u_i(\tau)\ \delta_{P,i,j}(\tau)$ in order to make it tractable to deal with MILP problem. Then this relationship can be equivalently represented as follows,

$$\begin{aligned}
-u_i(\tau) + \delta_{M,i,j}(\tau) &\leq 0, && (55)\\
-\delta_{P,i,j}(\tau) + \delta_{M,i,j}(\tau) &\leq 0, && (56)\\
u_i(\tau) + \delta_{P,i,j}(\tau) + \delta_{M,i,j}(\tau) &\leq 1. && (57)
\end{aligned}$$

Therefore, the MLDS description for the proposed system can be formalized as follows,

$$\begin{aligned}
\boldsymbol{x}(\kappa+1) &= \boldsymbol{A}\boldsymbol{x}(\kappa) + \boldsymbol{B}\boldsymbol{z}(\kappa), && (58)\\
\boldsymbol{z}(\kappa) &= \boldsymbol{C_1} diag(\boldsymbol{u}(\kappa))\boldsymbol{C_2}\boldsymbol{\delta}(\kappa), && (59)\\
\boldsymbol{E_2}\boldsymbol{\delta}(\kappa) &+ \boldsymbol{E_3}\boldsymbol{z}(\kappa) \\
&\leq \boldsymbol{E_1}\boldsymbol{u}(\kappa) + \boldsymbol{E_4}\boldsymbol{x}(\kappa) + \boldsymbol{E_5} && (60)
\end{aligned}$$

where the element $x_i(\kappa)$ of $\boldsymbol{x}(\kappa) \in \Re^{|P|}$, is marking of the place p_{c_i} at the sampling instance κ, the element $u_i(\kappa)(\in \{0,1\})$ of $\boldsymbol{u}(\kappa) \in Z^{|T|}$, is the signal of traffic light installed at ith district

and $\delta(\kappa)=[\delta_{\boldsymbol{P}}(\kappa),\ \delta_{\boldsymbol{M}}(\kappa)]'$. Note that if there is no traffic light installed at ith district, $u_i(\kappa)$ is always set to 1. And $\boldsymbol{A}$, $\boldsymbol{B}$, $\boldsymbol{C_1}$, $\boldsymbol{C_2}$, $\boldsymbol{E_1}$, $\boldsymbol{E_2}$, $\boldsymbol{E_3}$, $\boldsymbol{E_4}$ and $\boldsymbol{E_5}$ are the matrices with appropriate dimensions.

3.2 Model predictive control policy for traffic network control

The traffic system is large-scale dynamical system with uncertainty in the behavior of each car. In order to develop efficient traffic light control system, a wide range of traffic flow should be fully considered. In this subchapter, model predictive control policy for traffic light control is applied to the traffic flow model developed in the previous chapter. In RHC scheme, an input for next sampling period is decided based on the prediction for next several periods called the prediction horizon. This allows for the fact that the spatially changing dynamics of traffic flow are represented by temporal behavior over prediction horizon, since traffic flow can be considered as probabilistic time-series behavior.
The equation (58) can be modified, enumerating the state and input variables for the future periods as follows,

$$\begin{aligned}\boldsymbol{x}(\kappa+\lambda|\kappa) &= \boldsymbol{A^{\kappa}}x(\kappa)\\ &\quad+\sum_{\eta=0}^{\lambda-1}\{\boldsymbol{A^{\eta}}(\boldsymbol{BC_1}(diag(\boldsymbol{u}(\kappa+\lambda-1-\eta|\kappa)))\\ &\qquad\cdot\boldsymbol{C_2}\boldsymbol{\delta}(\kappa+\lambda-1-\eta|\kappa))\}\end{aligned} \tag{61}$$

where $x(\kappa+\lambda|\kappa)$ denotes the predicted state vector at time $\kappa+\lambda$, obtained by applying the input sequence $u(\lambda|\kappa)=u(\kappa),\cdots,u(\kappa+\lambda)$ to (58) starting from the state $x(\lambda|\kappa)=x(\kappa)$.
Now we consider following requirements that usually appear in the traffic light control problems.

(R1) Maximizes traffic flow over entire traffic network.

(R2) Avoid frequent change of traffic signal.

(R3) Avoid concentration of traffic flow in a certain district.

These requirements can be realized by minimizing the following objective function.

$$\begin{aligned}&J(\boldsymbol{u}(\lambda|\kappa),\cdots,\boldsymbol{u}(\lambda+N_I|\kappa)\\ &\quad,\boldsymbol{x}(\lambda|\kappa),\cdots,\boldsymbol{x}(\lambda+N_I|\kappa)\\ &\quad,\boldsymbol{\delta}(\lambda|\kappa),\cdots,\boldsymbol{\delta}(\lambda+N_I|\kappa))\\ &=\sum_{\lambda=1}^{N}\Bigg\{-\sum_i w_{1,i}\Bigg\{\Bigg(\boldsymbol{\Theta_i}\begin{bmatrix}x_i(\lambda|\kappa)/l_i\\ x_{i+1}(\lambda|\kappa)/l_{i+1}\end{bmatrix}\\ &\quad+\boldsymbol{\Phi}\Bigg)'\boldsymbol{\delta_{M,i}}(\lambda|\kappa)\Bigg\}\\ &\quad-\sum_i w_{2,i}\Big\{1-\big|u_i(\lambda|\kappa)-u_i(\lambda+1|\kappa)\big|\Big\}\\ &\quad+\sum_i w_{3,i}\Bigg\{\left|\frac{x_i(\lambda|\kappa)}{l_i}-\frac{x_{i+1}(\lambda|\kappa)}{l_{i+1}}\right|\Bigg\}\Bigg\}\end{aligned} \tag{62}$$